Silicon and Zinc Coordination to Peripheral Catechol Sites of (2,3,9,10,16,17,23,24-Octahydroxyphthalocyaninato)nickel(II). Phthalocyanine Coordination Chemistry at the Edge

Michael Ruf, Andrew M. Lawrence, Bruce C. Noll, and Cortlandt G. Pierpont*

Department of Chemistry and Biochemistry, University of Colorado, Boulder, Colorado 80309

Received January 13, 1998

(2,3,9,10,16,17,23,24-Octahydroxyphthalocyaninato)nickel(II) ($NiPc(OH)_8$) has been prepared by demethylation of (octamethoxyphthalocyaninato)nickel(II). Silylation of peripheral oxygen atoms using dimethyl-*tert*-butylsilyl chloride gave $NiPc(OSi(t\text{-}Bu)Me_2)_8$ as a convenient precursor to $NiPc(OH)_8$ with high solubility in hydrocarbon solvents. The coordination properties of peripheral catechol sites were investigated by treating $NiPc(OH)_8$ with $Tp^{Cum,Me}Zn(OH)$. A model study was first carried out by adding 5,6-dihydroxyphthalimide ($H_2PhtCat$) to $Tp^{Cum,Me}$-Zn(OH). Partial deprotonation occurred to give $Tp^{Cum,Me}Zn(HPhtCat)$. Further deprotonation with $NMe_4(OH)$ gave $(NMe_4)[Tp^{Cum,Me}Zn(PhtCat)]$ as the methanol solvate. ^1H NMR spectra recorded on $Tp^{Cum,Me}Zn(HPhtCat)$ show sharp resonances for equivalent arms of the $Tp^{Cum,Me}$ ligand, while $Tp^{Cum,Me}$ resonances for $(NMe_4)[Tp^{Cum,Me}$-Zn(PhtCat)] appear broadened by slow site exchange about the strongly chelated catecholate ligand. Similarly, the reaction between $NiPc(OH)_8$ and $Tp^{Cum,Me}Zn(OH)$ occurred with partial deprotonation to give $NiPc(OH)_4$-$(OZnTp^{Cum,Me})_4$. Structural characterization on crystals obtained from acetonitrile showed that Zn ions bond to single ring oxygen atoms at two sites and that they chelate to adjacent oxygen atoms at the other two ring sites. Cumenyl *i*-propyl substituents of the $Tp^{Cum,Me}$ ligands form hydrophobic pockets above and below the central metal of the phthalocyanine ring. These sites are occupied by acetonitrile solvent molecules positioned with hydrogen atoms directed toward the Ni atom in the crystal structure of the complex obtained by crystallization from a dichloromethane/acetonitrile solution. Addition of base to $NiPc(OH)_4(OZnTp^{Cum,Me})_4$ results in deprotonation of the remaining four OH groups and substantial red shifts for electronic transitions in the 400 and 600 nm regions of the phthalocyanine ring. Broadened ^1H NMR resonances for arms of the $Tp^{Cum,Me}$ ligands point to a chelated structure for the Zn atoms of $(NMe_4)_4[NiPc(O_2ZnTp^{Cum,Me})_4]$.

Introduction

Coordination complexes containing catecholate and semiquinonate radical ligands have been shown to exhibit unique properties of electron transfer, electrochemical activity, and magnetism.[1] We have been interested in extending this research to include compounds containing multiple metal−quinone units interacting through the conjugated structure of a planar macrocycle. Metallophthalocyanines have been chosen for this purpose due to their synthetic accessibility and chemical stability. The phthalocyanines are also among the most commercially significant metallomacrocycles with diverse applications that take advantage of their intense visible transitions and luminescent properties. These include use as dyes, nonlinear optical materials, mesophase liquid crystals, and photodynamic pharmaceuticals.[2,3]

In the solid state the phthalocyanines often form stacked lattices that result in low solubility. Bulky peripheral alkoxy substituents provide improved solubility, and uncomplicated synthetic procedures are available for octaalkoxyphthalocyanines with substituents at both ortho and para positions of the peripheral rings. Dealkylation of 2,3,9,10,16,17,23,24-octamethoxyphthalocyanine, $H_2Pc(OMe)_8$, has been used to form octahydroxyphthalocyanine, $H_2Pc(OH)_8$, obtained as a solid of low solubility.[4] The peripheral catechol groups of the ring should be highly effective chelating agents, and we now report the results of an initial investigation on the coordination chemistry of peripheral oxygen sites. With the importance of Pc electronic spectroscopy, it will be of interest to see if metals coordinated to atoms that are directly conjugated with ring π electronic levels can be used to give tunable and predictable shifts in optical transitions. Redox activity of the ring catechol functionalities will also be of interest. Oxidation of the parent phthalocyanine may occur in 10 e^-/proton transfer steps to give the fully oxidized phthalocyanine quinone (eq 1). Structural features of peripherally coordinated coligands may be used to create stereoselective pockets above and below the plane of the Pc ring, directing supramolecular axial binding at the central metal. For this investigation nickel(II) has been used as the central metal, and functionalized zinc pyrazolylborate units have been coordinated with peripheral catechol oxygen atoms.

(1) Pierpont, C. G.; Lange, C. W. *Prog. Inorg. Chem.* **1994**, *41*, 331.
(2) (a) *Phthalocyanines: Properties and Applications*; Leznoff, C. C., Lever, A. B. P., Eds.; VCH Publications: New York, 1989, Vol. I; 1992, Vol. II; 1993, Vol. III; 1996, Vol. IV. (b) Tran-Thi, T.-H. *Coord. Chem. Rev.* **1997**, *160*, 53.
(3) (a) Hanack, M.; Deger, S.; Lange, A. *Coord. Chem. Rev.* **1988**, *83*, 115. (b) Schultz, H.; Lehmann, H.; Rein, M.; Hanack, M. *Struct. Bonding* **1991**, *74*, 41.
(4) Leznoff, C. C.; Vigh, S.; Svirskaya, P. I.; Greengerg, S.; Drew, D. M.; Ben-Hur, E.; Rosenthal, I. *Photochem. Photobiol.* **1989**, *49*, 279.

S0020-1669(98)00036-6 CCC: $15.00
Published on Web 03/27/1998

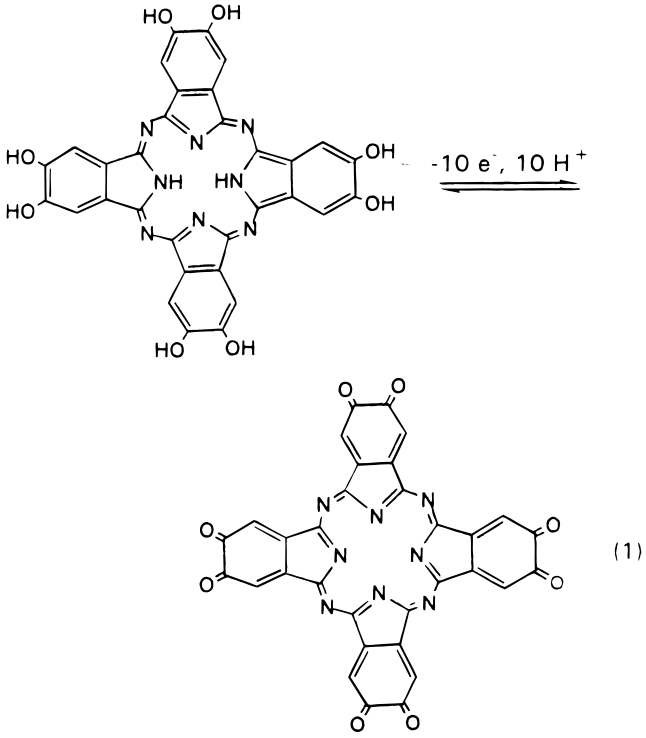

(1)

Experimental Section

Materials. 4,5-Dimethoxyphthalodinitrile was prepared from veratrole using a literature procedure.[5] $Tp^{Cum,Me}Zn(OH)$ was prepared by the procedure described by Ruf and Vahrenkamp.[6]

(2,3,9,10,16,17,23,24-Octamethoxyphthalocyaninato)nickel(II), NiPc(OMe)$_8$. 4,5-Dimethoxyphthalodinitrile (7.00 g, 37 mmol), urea (2.23 g, 37 mmol), $NiCl_2$ (1.12 g, 9.2 mmol), and a small quantity of ammonium molybdate were refluxed in 100 mL of ethylene glycol for 4 days. The mixture was cooled, and 100 mL of water was added. Filtration gave a dark blue precipitate as the crude product. The precipitate was washed with water and purified by Soxhlet extraction with acetone (24 h) and chloroform (24 h). $NiPc(OMe)_8$ was obtained in 68% yield (5.15 g).

^{1}H NMR (DMSO-d_6): δ 3.90 (s, 3H, OMe), 7.35 (s, 1H, CH).

Anal. Calcd for $C_{40}H_{24}N_8O_8Ni$: C, 59.8; H, 3.0; N, 14.0. Found: C, 60.1; H, 2.8; N, 14.2.

(2,3,9,10,16,17,23,24-Octahydroxyphthalocyaninato)nickel(II), NiPc(OH)$_8$. $NiPc(OMe)_8$ (5.15 g, 6.4 mmol) was suspended in 100 mL of dichloromethane, and BBr_3 (24 mL, 254 mmol) was added under N_2. The mixture was stirred for 15 days, and 100 mL of methanol was added slowly. The solvent was removed, 100 mL of MeOH was added to the residue, and this procedure was repeated three more times. $NiPc(OH)_8$ was separated from the MeOH by filtration, to give a dark green precipitate in 47% yield (2.1 g). The complex may be recrystallized from pyridine, giving dark green solvated crystals, $NiPc(OH)_8 \cdot 2NC_5H_5$.

^{1}H NMR (DMSO-d_6): δ 8.58 (s, 1H, CH), 10.37 (s (broad), 1H, OH).

Anal. Calcd for $C_{42}H_{26}N_{10}O_8Ni$: C, 58.8; H, 3.0; N, 16.3. Found: C, 58.1; H, 2.9; N, 15.6.

(2,3,9,10,16,17,23,24-Octakis(*tert*-butyldimethylsiloxy)phthalocyaninato)nickel(II), NiPc(OSi(*t*-Bu)Me$_2$)$_8$. $NiPc(OH)_8$ (0.50 g, 0.72 mmol), imidazole (0.40 g, 5.7 mmol), and $Si(t\text{-}Bu)(Me)_2Cl$ (1.00 g, 5.7 mmol) were dissolved in 150 mL of dichloromethane, and the mixture was stirred for 1 h. The volume of the solution was reduced under vacuum, and solid $NiPc(OSi(t\text{-}Bu)Me_2)_8$ was isolated by filtration in 71% yield (0.815 g). Dark green crystals suitable for crystallographic characterization were obtained by slow evaporation of a saturated chloroform solution. Crystals were found to form as the chloroform solvate, $NiPc(OSi(t\text{-}Bu)Me_2)_8 \cdot 2CHCl_3$.

^{1}H NMR ($CDCl_3$): δ 0.57 (s, 6H, Me), 1.20 (s, 9H, *t*-Bu), 8.76 (s, 1H, CH).

Anal. Calcd for $C_{82}H_{130}N_8O_8Cl_6Si_8Ni$: C, 53.1; H, 7.0; N, 6.0. Found: C, 52.2; H, 6.9; N, 5.7.

5,6-Dihydroxyphthalimide (H_2PhtCat). 4,5-Dimethoxyphthalodinitrile (1.00 g, 6.2 mmol) was dissolved in 50 mL of dichloromethane, and BBr_3 (15.9 g, 63.4 mmol) was added to the solution under N_2. The mixture was stirred for 2 days, and 50 mL of methanol was added slowly. Upon addition of 100 mL of water a yellow precipitate formed. The precipitate was isolated by filtration, washed with water, and recrystallized from ethanol. 5,6-Dihydroxyphthalimide was obtained in 74% yield (0.88 g).

$Tp^{Cum,Me}$Zn(HPhtCat). $Tp^{Cum,Me}ZnOH$ (200 mg, 0.29 mmol) was dissolved in 50 mL of dichloromethane. 5,6-Dihydroxyphthalimide (52 mg, 29 mmol) dissolved in 30 mL of methanol was added, and the mixture was slowly evaporated. Yellow crystals of $Tp^{Cum,Me}Zn(HPhtCat)$ were obtained in 84% yield (205 mg).

^{1}H NMR ($CDCl_3$): δ 1.07 (d, J = 6.9 Hz, 18H, Me(*i*-Pr)), 2.57 (s, 9H, Me(pz)), 2.68 (spt, J = 6.9 Hz, 3H, H(*i*-Pr)), 5.23 (s, 1H, NH), 6.21 (s, 3H, H(pz)), 6.82 (s, 1H, H(PhtCat)), 6.84 (s, 1H, OH), 6.95 (s, 1H, H(PhtCat)), 6.99 (d, J = 8.2 Hz, 6H, 3,5-H(Ph)), 7.43 (d, J = 8.2 Hz, 6H, 2,6-H(Ph)).

(NMe_4)[$Tp^{Cum,Me}$Zn(PhtCat)]. $Tp^{Cum,Me}Zn(HPhtCat)$ (50 mg, 0.06 mmol) was dissolved in 10 mL of dichloromethane, and 1 equiv of $NMe_4(OH)$ as a 1% methanol solution was added dropwise. The color of the solution turned to bright red-orange. The solvent was removed, and the residue was dissolved in 10 mL of methanol. Orange-red crystals separated from the solution upon cooling. The crystals were isolated by filtration and dried to give 46 mg of $(NMe_4)[Tp^{Cum,Me}Zn(PhtCat)]$ in 85% yield.

^{1}H NMR (CD_3CN): δ 1.12 (d, J = 6.9 Hz, 18H, Me(*i*-Pr)), 2.55 (s, 9H, Me(pz)), 2.79 (spt, J = 6.9 Hz, 3H, H(*i*-Pr)), 2.96 (s, 12H, NMe_4^+), 6.19 (s, 2H, H(PhtCat)), 6.29 (s, 3H, H(pz)), 7.02 (s (broad), 6H, 3,5-H(Ph)), 7.63 (d, J = 8.2 Hz, 6H, 2,6-H(Ph)).

Tetrakis[hydrotris(3-cumenyl-5-methylpyrazol-1-yl)boratozinc(II)](2,9,16,23-tetraoxo-3,10,17,24-tetrahydroxophthalocyaninato)nickel(II), NiPc(OH)$_4$(OZn$Tp^{Cum,Me}$)$_4$. $Tp^{Cum,Me}ZnOH$ (200 mg, 0.29 mmol) was dissolved in 100 mL of a 1:1 dichloromethane/methanol solution. $NiPc(OH)_8$ (51 mg, 0.07 mmol) was added to the solution, and the mixture was stirred until all of the $NiPc(OH)_8$ was dissolved (~12 h). The volume of the dark green solution was reduced to 50 mL under vacuum, and the dark green precipitate was separated by filtration, to give 110 mg of $NiPc(OH)_4(OZnTp^{Cum,Me})_4$ in 45% yield. Crystals used for crystallographic characterization were grown by slow diffusion of acetonitrile into a saturated dichloromethane solution of the complex and were obtained as the mixed solvate $NiPc(OH)_4(OZnTp^{Cum,Me})_4 \cdot 2CH_2Cl_2 \cdot 4.5CH_3CN$.

^{1}H NMR ($CDCl_3$): δ 0.39 (d, J = 6.9 Hz, 72H, Me(*i*-Pr)), 2.12 (spt, J = 6.9 Hz, 12H, H(*i*-Pr)), 2.73 (s, 36H, Me(pz)), 6.35 (s,12H, H(pz)), 6.73 (d, J = 8.2 Hz, 24H, 3,5-H(Ph)), 7.52 (s (broad), 4H, H(Pc)), 7.68 (d, J = 8.2 Hz, 24H, 2,6-H(Ph)), 8.36 (s (broad), 4H, H(Pc)).

(NMe_4)$_4$[NiPc(O_2Zn$Tp^{Cum,Me}$)$_4$]. $NiPc(OH)_4(OZnTp^{Cum,Me})_4$ (20 mg, 0.0059 mmol) was dissolved in 20 mL of dichloromethane. A 10% solution of $(NMe_4)OH$ in methanol (0.025 mL, 0.024 mmol) was added under N_2. The color of the solution turned from green to dark blue. A blue precipitate of $(NMe_4)_4[NiPc(O_2ZnTp^{Cum,Me})_4]$ formed in 64% yield (14 mg) upon addition of 20 mL of methanol.

^{1}H NMR ($CDCl_3$): δ 1.23 (d, J = 6.9 Hz, 72H, Me(*i*-Pr)), 2.58 (s, 36H, Me(pz)), 2.84 (spt, J = 6.9 Hz, 12H, H(*i*-Pr)), 3.04 (s, 64H, NMe_4^+), 6.4 (s (broad),12H, H(pz)), 6.9 (s (broad), 24H, 3,5-H(Ph)), 7.60 (d, J = 8.2 Hz, 24H, 2,6-H(Ph)), 8.26 (s, 8H, H(Pc)).

$(NMe_4)_4[NiPc(O_2ZnTp^{Cum,Me})_4]$ (10 mg, 0.0027 mmol) was dissolved in dichloromethane and treated with 1 M HCl (0.011 mL, 0.011 mmol). The solution turned green, and the product was identified spectroscopically as $NiPc(OH)_4(OZnTp^{Cum,Me})_4$.

Physical Methods. Electronic spectra were recorded on a Perkin-Elmer Lambda 9 spectrophotometer. Infrared spectra were recorded

(5) Metz, J.; Schneider, O.; Hanack, M. *Inorg. Chem.* **1984**, *23*, 1065.
(6) (a) Ruf, M.; Vahrenkamp, H. *Inorg. Chem.* **1996**, *35*, 6571. (b) Ruf, M.; Burth, R.; Weis, K.; Vahrenkamp, H. *Chem. Ber.* **1996**, *129*, 1251. (c) Ruf, M.; Weis, K.; Brasack, I.; Vahrenkamp, H. *Inorg. Chim. Acta* **1996**, *250*, 271.

Table 1. Crystallographic Data for $NiPc(OSi(t\text{-}Bu)Me_2)_8 \cdot 2CHCl_3$, $ZnTp^{Cum,Me}(HPhtCat) \cdot MeOH \cdot 1.5CH_2Cl_2$, $(NMe_4)[ZnTp^{Cum,Me}(PhtCat)] \cdot 2.75MeOH$, and $NiPc(OH)_4(OZnTp^{Cum,Me})_4 \cdot 3CH_3CN$[a]

	$NiPc(OSi(t\text{-}Bu)Me_2)_8$	$ZnTp^{Cum,Me}(HPhtCat)$	$(NMe_4)[ZnTp^{Cum,Me}(PhtCat)]$	$NiPc(OH)_4(OZnTp^{Cum,Me})$
formula	$C_{82}H_{130}Cl_6N_8O_8Si_8Ni$	$C_{49.5}H_{59}Cl_3BN_7O_5Zn$	$C_{53.75}H_{64}BN_8O_{6.75}Zn$	$C_{194}H_{205}B_4N_{35}O_8NiZn_4$
fw	1852.1	1011.5	1014.4	3518.4
space group	$P2_1/c$	$Pbca$	$P2_1/c$	$P\bar{1}$
a (Å)	14.4045(2)	21.043(2)	16.623(5)	18.664(5)
b (Å)	23.1604(3)	16.378(2)	14.197(3)	17.566(5)
c (Å)	15.4997(2)	29.347(4)	24.602(5)	18.708(7)
α (deg)	90	90	90	110.78(3)
β (deg)	100.799(1)	90	106.781(15)	116.59(3)
γ (deg)	90	90	90	96.35(2)
vol ($Å^3$)	5079.34(12)	10 114(2)	5559(2)	4854(3)
Z	2	8	4	1
T (K)	141	166	171	161
λ (Mo Ka, Å)	0.710 73	0.710 73	0.710 73	0.710 73
D_{calcd} (g cm^{-3})	1.211	1.329	1.212	1.204
m (mm^{-1})	0.495	0.696	0.497	0.646
R, R_w	0.046, 0.109[b]	0.057, 0.138	0.060, 0.154	0.084, 0.220

[a] Details of the structure determination of $NiPc(OH)_4(OZnTp^{Cum,Me})_4 \cdot 4.5CH_3CN \cdot 2CH_2Cl_2$ are given in the Supporting Information. [b] $R = \sum||F_o| - |F_c||/\sum|F_o|$. $R_w = [\sum w(F_o^2 - F_c^2)^2/\sum wF_o^4]^{1/2}$.

on a Perkin-Elmer 1600 FTIR with samples prepared as KBr pellets. ^1H NMR spectra were recorded on a Varian VXR 300s spectrometer.

Crystallographic Structure Determination on $NiPc(OSi(t\text{-}Bu)Me_2)_8 \cdot 2CHCl_3$. Dark green crystals were obtained by slow evaporation of a chloroform solution. A sphere of intensity data was collected at 141 K using a Siemens SMART system equipped with a CCD detector. Crystals obtained from chloroform form in the monoclinic crystal system, space group $P2_1/c$, in a unit cell of the dimensions given in Table 1. Direct methods were used to solve the structure. The Ni atom is located at a crystallographic inversion center in the unit cell. A difference Fourier calculated with all non-hydrogen atoms of the molecule indicated the location of a chloroform molecule of solvation at a general position in the unit cell. Refinement converged with $R(F) = 0.046$ and $R_w(F^2) = 0.109$.

Crystallographic Structure Determination on $Tp^{Cum,Me}Zn(HPhtCat) \cdot CH_3OH \cdot 1.5CH_2Cl_2$. A yellow needle of $Tp^{Cum,Me}Zn(HPhtCat)$ obtained by recrystallization from a dichloromethane/methanol solution was mounted and aligned on a Siemens SMART system equipped with a CCD detector. A sphere of intensity data was collected at 166 K. Crystals were found to form in the orthorhombic crystal system, space group *Pbca*, in a unit cell of dimensions given in Table 1. The structure was solved by direct methods. A difference Fourier calculated using the phases provided by atoms of the complex molecule was used to locate the atoms of the solvate molecules. Final refinement converged with $R(F) = 0.057$ and $R_w(F^2) = 0.137$.

Crystallographic Structure Determination on $(NMe_4)[Tp^{Cum,Me}Zn(PhtCat)] \cdot 2.75CH_3OH$. An orange-red plate of $(NMe_4)[Tp^{Cum,Me}Zn(PhtCat)]$ obtained by recrystallization from a methanol solution was mounted and aligned on a Siemens SMART system equipped with a CCD detector. A sphere of intensity data was collected at 171 K. Crystals were found to form in the monoclinic crystal system, space group $P2_1/c$, in a unit cell of the dimensions given in Table 1. The structure was solved by direct methods. A difference Fourier calculated using the phases provided by atoms of the complex molecule was used to locate the atoms of the solvate molecules. Final refinement converged with $R(F) = 0.060$ and $R_w(F^2) = 0.154$.

Crystallographic Structure Determination on $NiPc(OH)_4(OZnTp^{Cum,Me})_4 \cdot 3CH_3CN$. Dark green crystals of $NiPc(OH)_4(OZnTp^{Cum,Me})_4$ were obtained from an acetonitrile solution. A sphere of intensity data was collected at 161 K using a Siemens SMART system equipped with a CCD detector. Crystals were found to form in the triclinic crystal system, space group $P\bar{1}$, in a unit cell of the dimensions given in Table 1. Direct methods were used to solve the structure. The central Ni atom is located at a crystallographic inversion center of the unit cell. A difference Fourier calculated with the atoms of $NiPc(OH)_4(OZnTp^{Cum,Me})_4$ indicated the presence of the acetonitrile molecules of solvation. Final refinement converged with $R(F) = 0.084$ and $R_w(F^2) = 0.220$.

Crystallographic Structure Determination on $NiPc(OH)_4(OZnTp^{Cum,Me})_4 \cdot 2CH_2Cl_2 \cdot 4.5CH_3CN$. Dark green crystals of $NiPc(OH)_4(OZnTp^{Cum,Me})_4$ were obtained from a dichloromethane/acetonitrile solution. A sphere of intensity data was collected at 161 K using a Siemens SMART system equipped with a CCD detector. Crystals were found to form in the triclinic crystal system, space group $P\bar{1}$, in a unit cell of the dimensions given in the Supporting Information. Direct methods were used to solve the structure. The central Ni atom is located at a crystallographic inversion center of the unit cell. A difference Fourier calculated with the atoms of $NiPc(OH)_4(OZnTp^{Cum,Me})_4$ indicated the presence of both dichloromethane and acetonitrile molecules of solvation. Ordered acetonitrile molecules were found at an axial site above the Ni and hydrogen bonded to the proton of O2. The remaining acetonitrile and dichloromethane molecules are located in a large void in the unit cell. Their disorder and fractional occupancy have limited the precision of the structure determination. Refinement converged with $R = 0.111$.

Results and Discussion

Considerable research has been directed at the synthesis of polycatechol ligands for use as chelating agents that exhibit metal-ion selectivity and high kinetic stability.[7] With appropriate flexibility in the ligand backbone the catechol functionalities encapsulate a single metal ion. The four sets of catecholate oxygens of 2,3,9,10,16,17,23,24-octahydroxyphthalocyanine ($H_2Pc(OH)_8$) are positioned to chelate with four separate metal ions, with a fifth metal occupying the central N_4 chelation site of the heterocycle. In this respect, $MPc(OH)_8$, where M is the central metal ion, resembles the tetradithiolate star-porphyrazine ligand of Barrett and Hoffman.[8] Drawing from synthetic procedures used by Raymond in the synthesis of tris(catechol) chelating ligands[9] and Leznoff's synthesis of $H_2Pc(OH)_8$,[4] BBr_3/MeOH dealkylation has been used to prepare $NiPc(OH)_8$ beginning with (octamethoxyphthalocyaninato)nickel(II), $NiPc(OMe)_8$. Octamethoxyphthalocyanines may be conveniently prepared with a variety of central metal ions,[4,5] and this procedure should prove to be a general route to a series of MPc-

(7) Matzanke, B. F.; Müller-Matzanke, G.; Raymond, K. N. In *Iron Carriers and Iron Proteins*; Loehr, T. M., Ed.; Physical Bioinorganic Chemistry Series; VCH Publishers: New York, 1989; pp 1−121.

(8) (a) Velázquez, C. S.; Fox, G. A.; Broderick, W. E.; Andersen, K. A.; Anderson, O. P.; Barrett, A. G. M.; Hoffman, B. M. *J. Am. Chem. Soc.* **1992**, *114*, 7416. (b) Velázquez, C. S.; Baumann, T. F.; Olmstead, M. M.; Hope, H.; Barrett, A. G. M.; Hoffman, B. M. *J. Am. Chem. Soc.* **1993**, *115*, 9997.

(9) Karpishin, T. B.; Stack, T. D. P.; Raymond, K. N. *J. Am. Chem. Soc.* **1993**, *115*, 6115.

Table 2. Electronic Transitions of $NiPc(OH)_8$, $NiPc(OSi(t\text{-}Bu)Me_2)_8$, $NiPc(OH)_4(OZnTp^{Cum,Me})_4$, and $(NMe_4)_4[NiPc(O_2ZnTp^{Cum,Me})_4]$

compound	UV−vis−NIR (λ_{max}, nm)
$NiPc(OH)_8$	290, 320, 420, 613, 650, 680
$NiPc(OSi(t\text{-}Bu)Me_2)_8$	305, 325, 400, 609, 650, 670
$NiPc(OH)_4(OZnTp^{Cum,Me})_4$	230, 240, 301, 320, 445, 618, 660, 688
$(NMe_4)_4[NiPc(O_2ZnTp^{Cum,Me})_4]$	230, 269, 324, 563, 740

$(OH)_8$ complexes using relatively simple synthetic methods. The electronic spectrum of $NiPc(OH)_8$ consists of the six transitions that are commonly observed for metallophthalocyanines in the region between 250 and 800 nm (Table 2).[10]

$NiPc(OSi(t\text{-}Bu)(Me)_2)_8$. As might be expected, $NiPc(OH)_8$ has low solubility in most solvents of low polarity. Ring oxygen atoms were silylated using $Si(t\text{-}Bu)(Me)_2Cl$ to give $NiPc(OSi(t\text{-}Bu)(Me)_2)_8$ (eq 2). Octasilyloxylated phthalocyanines are

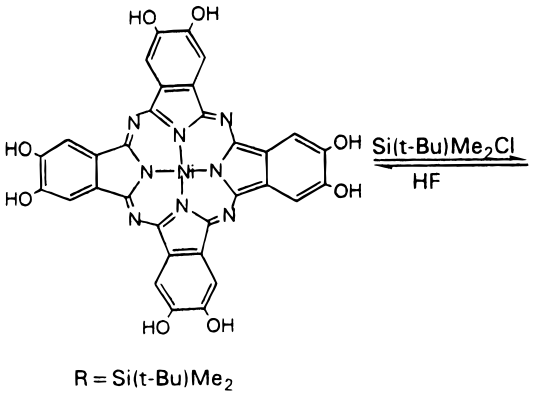

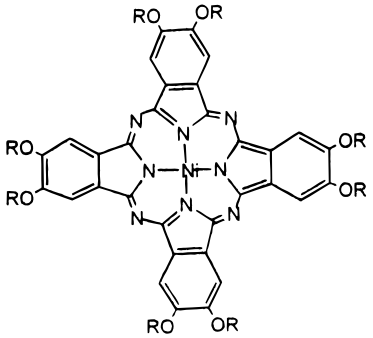

(2)

highly unusual; there appear to be no references to compounds of this type in the open chemical literature.[11] They should prove to be useful precursors to peripherally functionalized phthalocyanines, but for present purposes, the solubility of $NiPc(OSi(t\text{-}Bu)(Me)_2)_8$ in hydrocarbon solvents makes it a useful precursor to $NiPc(OH)_8$ by treatment with HF or with metal fluorides. Crystals of $NiPc(OSi(t\text{-}Bu)(Me)_2)_8 \cdot 2CHCl_3$ obtained by slow evaporation of a saturated chloroform solution were used for structural characterization to confirm the composition of the compound and to provide metrical features of the catecholate functionalities. A view of the molecule is shown in Figure 1; selected bond lengths and angles are listed in Table 3. Catecholate C−O lengths average to 1.374(3) Å, and the

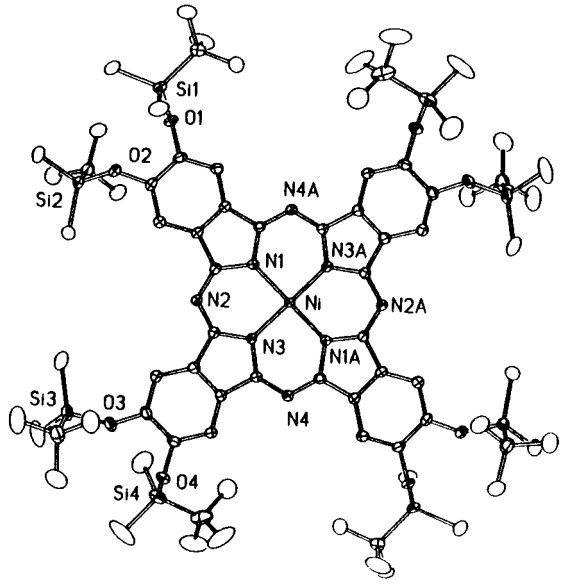

Figure 1. View of the $NiPc(OSi(t\text{-}Bu)Me_2)_8$ molecule.

Table 3. Selected Bond Lengths and Angles for $NiPc(OSi(t\text{-}Bu)Me_2)_8$

	Bond Lengths (Å)		
Ni−N1	1.906(2)	Ni−N3	1.902(2)
N1−C1	1.386(3)	N1−C8	1.389(3)
C1−C2	1.450(3)	C2−C7	1.390(3)
C7−C8	1.457(3)	N2−C8	1.324(3)
N2−C9	1.326(3)	N3−C9	1.387(3)
N3−C16	1.382(3)	C9−C10	1.457(3)
C10−C15	1.394(3)	C15−C16	1.455(3)
N4−C16	1.323(3)	C4−C5	1.427(4)
O1−C4	1.370(3)	O2−C5	1.376(3)
C2−C3	1.401(3)	C3−C4	1.384(4)
C5−C6	1.387(4)	C6−C7	1.402(4)
C10−C11	1.399(4)	C11−C12	1.390(4)
C12−C13	1.428(3)	C13−C14	1.383(4)
C14−C15	1.395(3)	C10−C15	1.394(3)
O3−C12	1.368(3)	O4−C13	1.381(3)
Si1−O1	1.676(2)	Si4−O4	1.680(2)
Si2−O2	1.680(2)	Si3−O3	1.673(2)
	Angles (deg)		
N1−Ni−N3	89.76(8)	N1−Ni−N3′	90.24(8)
C8−N2−C9	120.5(2)	C16−N4−C1′	120.6(2)
Si1−O1−C4	128.9(2)	Si2−O2−C5	129.4(2)
Si3−O3−C12	135.3(2)	Si4−O4−C13	125.0(2)

C−C bond between oxygen atoms is the longest of the Cat benzene ring with an average value of 1.428(3) Å. The other C−C bond to these carbon atoms is the shortest ring length, for both independent rings, with an average value of 1.386(3) Å.

$ZnTp^{Cum,Me}(HPhtCat)$. The chelation properties of peripheral catecholate oxygens of $NiPc(OH)_8$ have been investigated using a complex of zinc. Zinc catecholate complexes are optically transparent in the region of the phthalocyanine electronic transitions, and ^1H NMR may be used for characterization. The specific zinc complex used for this purpose is $Tp^{Cum,Me}Zn(OH)$, a complex developed by Ruf and Vahrenkamp for studies on the hydrolytic cleavage of protic substrate molecules at an encapsulated pocket.[6] When treated with 3,5-di-*tert*-butylcatechol in air, $Tp^{Cum,Me}Zn(OH)$ was found to give $Tp^{Cum,Me}Zn(3,5\text{-}DBSQ)$ (**I**), containing the partially oxidized radical semiquinonate ligand.[12] The $Tp^{Cum,Me}Zn$ pocket is large enough to accommodate the 3,5-DBSQ ligand, and aerobic

(10) (a) Guo, L.; Ellis, D. E.; Hoffman, B. M.; Ishikawa, Y. *Inorg. Chem.* **1996**, *35*, 5304. (b) Liang, X. L.; Flores, S.; Ellis, D. E.; Hoffman, B. M.; Musselman, R. L. *J. Chem. Phys.* **1991**, *95*, 403.

(11) References to phthalocyanine compounds containing bulky silyl groups appear in the patent literature on laser optical recording media. See, for example: (a) Tomura, T.; Sato, T.; Sasa, N.; Maruyama, K.; Nakajima, S.; Yashiro, T. Japanese Patent 07 89,240, 1995. (b) Tomura, T.; Sato, T.; Sasa, N. Japanese Patent 07,156,550, 1995.

(12) Ruf, M.; Noll, B. C.; Groner, M.; Yee, G. T.; Pierpont, C. G. *Inorg. Chem.* **1997**, *36*, 4860.

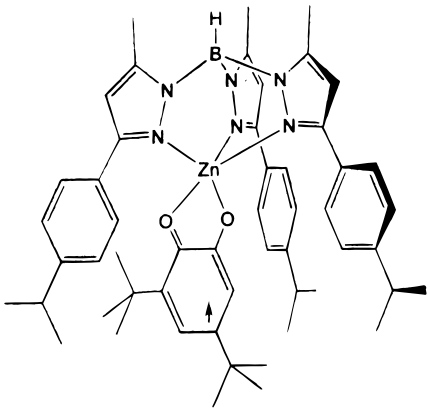

(I)

oxidation of the catecholate species formed initially in the reaction is accompanied by complete deprotonation of the quinone ligand. A related reaction was carried out beginning with 5,6-dihydroxyphthalimide (H_2PhtCat, **II**) as a simple model

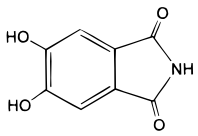

(II)

for coordination to peripheral catecholate sites of NiPc(OH)$_8$. In the absence of additional base, deprotonation of the catechol oxygens of H_2PhtCat by Tp^{Cum,Me}Zn(OH) was found to occur stoichiometrically to give the partially protonated catecholate complex Tp^{Cum,Me}Zn(HPhtCat). The results of structural characterization on this product are shown in Figure 2, with selected bond lengths and angles listed in Table 4. The geometry about the Zn atom is trigonal bipyramidal, with N1 and protonated oxygen O2 occupying axial sites. Equatorial Zn−N lengths to N2 and N3 are shorter (2.050(3) Å) than the axial Zn−N1 length of 2.102(3) Å, and the equatorial Zn−O1 length of 1.912(2) Å is considerably shorter than the axial Zn−O2 length of 2.292(2) Å. Values for the protonated and deprotonated C−O lengths are quite different, with significant double bond character for the O1−C40 length of 1.302(4) Å and a normal single bond length of 1.357(3) Å for the O2−C41 bond to the protonated oxygen. The C40−C41 length between catecholate oxygens is 1.428(4) Å, similar to ring values at this position for NiPc(OSi(*t*-Bu)(Me)$_2$)$_8$, but the C40−C45 and C41−C42 lengths differ with the longer of the two to the carbon atom with the shortest C−O length, C40. As a further consequence, the outer ring C−C lengths also show a short/long pattern with the shortest to C45.

The crystal structure of Tp^{Cum,Me}Zn(HPhtCat) consists of polymeric strands of complex molecules linked by hydrogen bonding between the hydrogen atom bonded to O2 and oxygen O8 of an adjacent molecule.

Cumenyl phenyl rings of equatorial nitrogens N2 and N3 of the Tp^{Cum,Me} ligand are stacked on either side of the catecholate ligand, but despite this environmental difference in the solid state, arms of the pyrazolylborate show structural equivalence in solution. ^{1}H NMR spectra show a single sharp doublet for the cumenyl isopropyl groups and a well-resolved septet for the methine hydrogen. However, with the equivalence of arms of the Tp^{Cum,Me} ligand, proton resonances for the two ring protons of the phthalimide ligand appear separately at 6.82 and 6.84 ppm. A reasonable explanation for the NMR spectrum is that protonated oxygen O2 dissociates from the Zn in solution to give a tetrahedral species that is responsible for the symmetrical environment of the Tp^{Cum,Me} ligand.

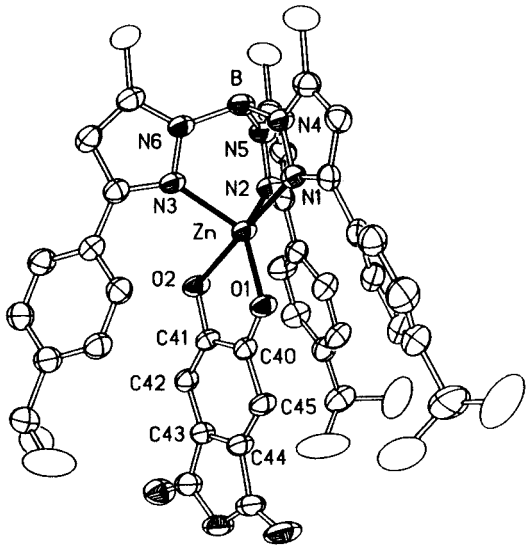

Figure 2. View of the ZnTp^{Cum,Me}(HPhtCat) molecule, including the proton bonded to oxygen O2. Structural features of the [ZnTp^{Cum,Me}(PhtCat)]$^-$ anion are similar, with differences in the disposition of isopropyl carbon atoms of the cumenyl groups and a shorter Zn−O2 length.

Table 4. Selected Bond Lengths and Angles for ZnTp^{Cum,Me}(HPhtCat) and [ZnTp^{Cum,Me}(PhtCat)]$^-$

	ZnTp^{Cum,Me}(HPhtCat)	[ZnTp^{Cum,Me}(PhtCat)]$^-$
	Bond Lengths (Å)	
Zn−O1	1.912(2)	1.979(2)
Zn−O2	2.292(2)	2.054(2)
Zn−N1	2.102(3)	2.186(2)
Zn−N2	2.045(3)	2.101(2)
Zn−N3	2.055(3)	2.089(2)
O1−C40	1.302(4)	1.327(2)
O2−C41	1.357(3)	1.312(2)
C40−C41	1.428(4)	1.447(3)
C40−C45	1.406(4)	1.399(3)
C41−C42	1.374(4)	1.401(3)
C42−C43	1.392(4)	1.392(3)
C43−C44	1.385(4)	1.392(3)
C44−C45	1.374(5)	1.394(3)
C43−C47	1.476(5)	1.472(3)
C44−C46	1.466(4)	1.474(3)
C47−O9	1.207(4)	1.219(3)
C46−O8	1.219(4)	1.216(3)
N7−C46	1.380(5)	1.395(3)
N7−C47	1.409(4)	1.394(3)
	Angles (deg)	
N1−Zn−O2	177.0(1)	170.60(7)
N2−Zn−N3	93.0(1)	94.71(7)
O1−Zn−N2	130.3(1)	140.53(8)
O1−Zn−N3	132.5(1)	124.55(7)
N2−Zn−O2	88.7(1)	97.25(6)
O1−Zn−O2	85.3(1)	82.35(6)
O2−Zn−N3	88.6(1)	98.19(7)
N1−Zn−N2	88.7(1)	82.77(7)
N1−Zn−N3	93.1(1)	91.17(8)
O1−Zn−N1	104.7(1)	91.65(6)

The difference between the chemistry of Tp^{Cum,Me}Zn(OH) with H_2(3,5-DBCat) and with H_2PhtCat is related to the influence that substituents have on catechol oxidation potential. Aerobic oxidation occurs readily for 3,5-DBCat, but the electron-withdrawing effect of the phthalimide functionality results in a more positive oxidation potential for Tp^{Cum,Me}Zn-

(HPhtCat). Consequently, the partially protonated species that forms initially in the reaction between $Tp^{Cum,Me}Zn(OH)$ and H_2(3,5-DBCat) undergoes rapid aerobic oxidation to $Tp^{Cum,Me}$-Zn(3,5-DBSQ), while $Tp^{Cum,Me}Zn$(HPhtCat), and even the $[Tp^{Cum,Me}Zn(PhtCat)]^-$ anion, are stable in air.

$(NMe_4)[Tp^{Cum,Me}Zn(PhtCat)]$. Deprotonation of the remaining catechol hydrogen of $Tp^{Cum,Me}Zn$(HPhtCat) with NMe_4-(OH) is accompanied by a color change, from yellow to the bright orange-red color of $(NMe_4)[Tp^{Cum,Me}Zn(PhtCat)]$. Crystallographic characterization was carried out to compare the features of the chelated catecholate ligand with the partially protonated ligand of $Tp^{Cum,Me}Zn$(HPhtCat). The trigonal bipyramidal geometry of $Tp^{Cum,Me}Zn$(HPhtCat) is conserved (Figure 2) with the catecholate oxygen O2, formerly the protonated oxygen, and pyrazolylborate nitrogen N1 occupying axial coordination sites. Bond lengths (Table 4) to the Zn at equatorial sites are shorter than axial lengths. The Zn−O2 length is contracted from 2.292(2) Å for the protonated ligand to 2.054(2) Å for $[Tp^{Cum,Me}Zn(PhtCat)]^-$. Strong donation to the metal by the chelated catecholate ligand results in general lengthening of all Zn−O and Zn−N lengths, relative to $Tp^{Cum,Me}Zn$(HPhtCat). The Zn−O1 length is 1.979(2) Å, 0.07 Å longer than the value of $Tp^{Cum,Me}Zn$(HPhtCat), and equatorial Zn−N lengths are roughly 0.05 Å longer for the anion. As would be expected, features of the PhtCat ligand are more symmetrical than the C−O and ring C−C lengths of HPhtCat. Both C−O lengths, 1.312(2) and 1.327(2) Å, are relatively short for a catecholate as a consequence of the Lewis acidic character of the Zn. The C40−C41 ring bond between the oxygens is long for an aromatic length (1.447(3) Å), but other ring C−C lengths are within the range of aromatic values.

The ^{1}H NMR spectrum of the $[Tp^{Cum,Me}Zn(PhtCat)]^-$ anion has features that indicate site exchange for the $Tp^{Cum,Me}$ ligand, but on a time scale that is slower than the exchange process of $Tp^{Cum,Me}Zn$(HPhtCat). Ring protons of the HPhtCat ligand appeared as separate resonances at 6.82 and 6.95 ppm, while for the deprotonated PhtCat ligand they appear as a single broad resonance at 6.19 ppm. All of the resonances for the arms of the $Tp^{Cum,Me}$ ligand are broadened relative to the spectrum of $Tp^{Cum,Me}Zn$(HPhtCat), but the difference appears most significantly for the aromatic ring protons at the 3 and 5 ring positions of the cumenyl rings. These appear as a sharp doublet at 6.99 ppm for $Tp^{Cum,Me}Zn$(HPhtCat), but as a broad singlet at 7.02 ppm for $[Tp^{Cum,Me}Zn(PhtCat)]^-$. The process that averages the resonances of arms of the $Tp^{Cum,Me}$ ligand and ring protons of PhtCat is slower for the deprotonated catecholate ligand. It may involve either dynamic exchange of axial and equatorial sites of $[Tp^{Cum,Me}Zn(PhtCat)]^-$ without ligand dissociation or, possibly, slow dissociation of the axial catecholate oxygen to form a tetrahedral Zn intermediate. It may be expected that dissociation of the deprotonated oxygen would be slower than for the protonated oxygen of $Tp^{Cum,Me}Zn$(HPhtCat).

$NiPc(OH)_4(OZnTp^{Cum,Me})_4$. Reactions were carried out between $NiPc(OH)_8$ and 4 equiv of $Tp^{Cum,Me}Zn(OH)$ to investigate the coordination properties of ring catechol functionalities. Solvated crystals of the reaction product were obtained by recrystallization either from acetonitrile or from an acetonitrile/dichloromethane mixture. Crystals obtained from both media were investigated crystallographically. Structural features of the complex molecule were the same, but difficulties in treating disorder of the solvate molecules provided a less satisfactory result for crystals of the mixed solvate. The product $NiPc(OH)_4$-$(OZnTp^{Cum,Me})_4$, shown in Figure 3, results from stoichiometric

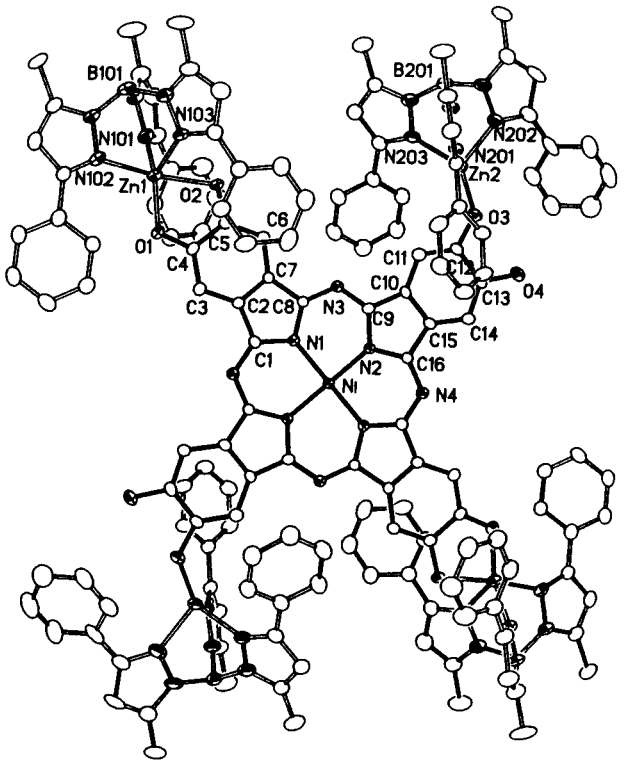

Figure 3. View of $NiPc(OH)_4(OZnTp^{Cum,Me})_4$. Isopropyl groups of the $Tp^{Cum,Me}$ ligands have been omitted for clarity.

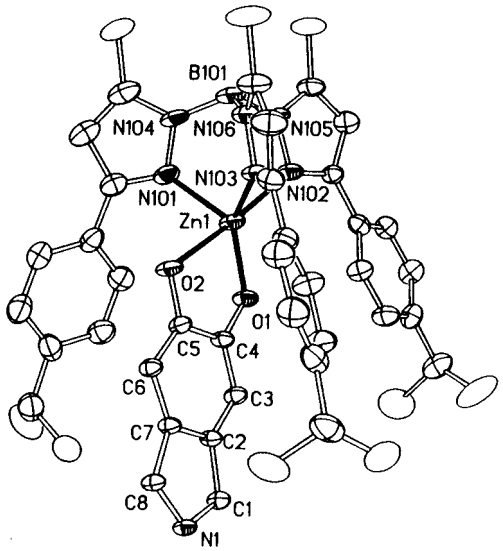

Figure 4. A view of the coordination environment of Zn1. O2 is the protonated oxygen atom.

deprotonation of half of the catechol oxygens in a reaction that is similar to reaction with H_2PhtCat. Zinc atoms are chelated unsymmetrically by oxygens of two trans catechols (Figure 4) and bond to single deprotonated Cat oxygens at the remaining two sites of the centrosymmetric ring (Figure 5). Structural features (Table 5) at the chelated sites are similar to those of $ZnTp^{Cum,Me}$(HPhtCat), and the sites of tetrahedral Zn coordination likely resemble the dissociated form of $Tp^{Cum,Me}Zn$-(HPhtCat) that exists in solution. At the chelated site Zn1 is coordinated unsymmetrically to O1 and protonated oxygen O2, with metrical values for the catechol region of the phthalocyanine ligand that resemble the features of the model complex $ZnTp^{Cum,Me}$(HPhtCat). The Zn2−O3 length, at the site where coordination is to a single oxygen, is quite short, 1.865(4) Å,

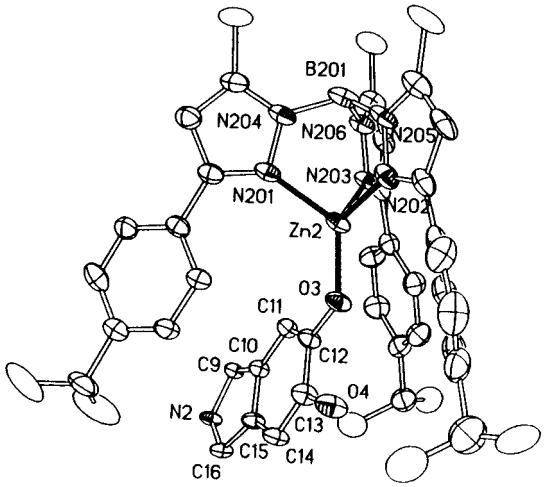

Figure 5. A view of the Zn2 coordination geometry.

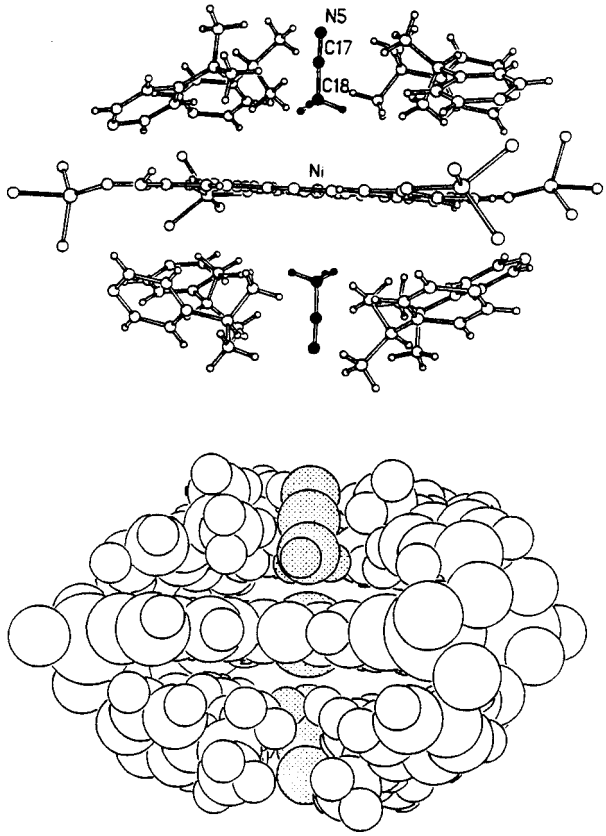

Figure 6. Views of the hydrophobic pockets above and below the Ni atom containing acetonitrile molecules. The orientation of the acetonitrile molecule was determined from the C−C (1.35(2) Å) and C≡N (1.12(2) Å) bond lengths, and the Ni−C18 separation is 3.34 Å.

only slightly longer than the Zn−O length of $ZnTp^{Cum,Me}(OH)$ (1.847(4) Å).[6a] Even with the structural complexity of $NiPc(OH)_4(OZnTp^{Cum,Me})_4$ its ^1H NMR spectrum closely resembles that of $ZnTp^{Cum,Me}$(HPhtCat). Rapid site exchange averages arms of the $Tp^{Cum,Me}$ ligands to give a sharp doublet for cumenyl isopropyl protons and a well-resolved septet for the isopropyl methine proton, both shifted upfield relative to $ZnTp^{Cum,Me}$(HPhtCat). The phthalocyanine ring protons appear as two broadened resonances at 7.52 and 8.36 ppm resulting from asymmetry in coordination to the partially protonated catechol functionalities. As with $ZnTp^{Cum,Me}$(HPhtCat), dissociation at the Zn1−O2 bond would account for both $Tp^{Cum,Me}$ exchange and the environmental differences for the Pc ring protons.

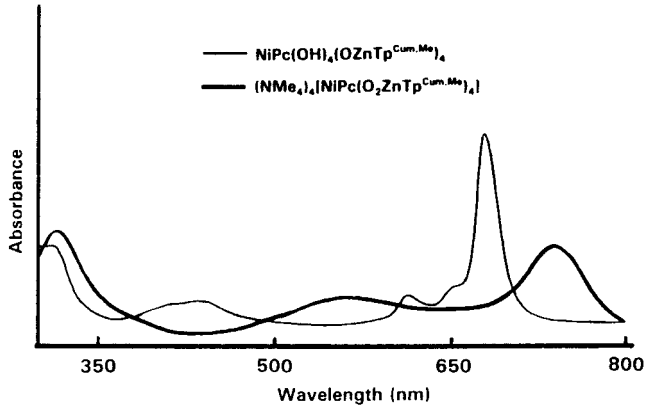

Figure 7. Changes in electronic spectrum (CH_2Cl_2) that occur with the addition of $(NMe_4)OH$ to $NiPc(OH)_4(OZnTp^{Cum,Me})_4$.

Table 5. Selected Bond Lengths and Angles for $NiPc(OH)_4(OZnTp^{Cum,Me})_4$

Bond Lengths (Å)			
Ni−N1	1.905(4)	Ni−N2	1.903(4)
N1−C1	1.372(7)	N1−C8	1.375(6)
N2−C9	1.381(6)	N2−C16	1.377(7)
N3−C8	1.324(7)	N3−C9	1.326(7)
N4−C16	1.320(7)	N4−C1′	1.332(7)
C4−C5	1.446(8)	O1−C4	1.321(7)
O2−C5	1.325(6)	C12−C13	1.423(8)
O3−C12	1.352(6)	O4−C13	1.385(7)
Zn1−O1	1.915(4)	Zn1−O2	2.264(4)
Zn1−N101	2.034(6)	Zn1−N102	2.159(6)
Zn1−N103	2.063(5)	Zn2−O3	1.865(4)
Zn2−N201	2.046(6)	Zn2−N202	2.017(5)
Zn2−N203	2.028(5)		
Angles (deg)			
N1−Ni−N2	89.6(2)	N1−Ni−N2′	90.4(2)
C8−N3−C9	121.7(5)	C16−N4−C1′	120.2(5)
N102−Zn1−O1	108.9(2)	N102−Zn1−N101	92.6(2)
N102−Zn1−N103	85.4(2)	N101−Zn1−N103	96.9(2)
O1−Zn1−N101	127.0(2)	O1−Zn1−N103	131.6(2)
N201−Zn2−N202	94.1(2)	N202−Zn2−N203	92.6(2)
N201−Zn2−N203	94.0(2)	O3−Zn2−N201	124.8(2)
O3−Zn2−N202	117.0(2)	O3−Zn2−N203	125.9(2)

Crystals of $NiPc(OH)_4(OZnTp^{Cum,Me})_4$ grown from a dichloromethane/acetonitrile solution were obtained as a mixed solvate. A cluster consisting of both CH_2Cl_2 and CH_3CN molecules was found to be located in a large void in the crystal structure near the cumenyl groups directed away from the catecholate rings in Figure 3. Fractional occupancy and disorder of these molecules have limited the precision of this structure determination so that it is less precise than the result obtained for the acetonitrile solvate alone. An interesting feature of this solvate is the presence of a pair of ordered acetonitrile molecules located above and below the central Ni atom in a hydrophobic pocket created by cumenyl isopropyl groups. They are directed toward the center of the phthalocyanine ring (Figure 6) with methyl protons, rather than the nitrogen, pointing toward the Ni. This feature demonstrates how the ligands of peripherally coordinated metal ions may be used to influence the stereochemistry at axial coordination sites about the central metal ion.

$(NMe_4)_4[NiPc(O_2ZnTp^{Cum,Me})_4]$. The addition of 4 equiv of $(NMe_4)OH$ to a solution of $NiPc(OH)_4(OZnTp^{Cum,Me})_4$ was used to completely deprotonate peripheral oxygen atoms. The O−H stretching vibration that appears at 3409 cm^{-1} for $NiPc(OH)_4(OZnTp^{Cum,Me})_4$ disappeared as expected, and the B−H vibration at 2545 cm^{-1} shifted slightly to 2535 cm^{-1}. Intense transitions that appear at 445 and 688 nm for $NiPc(OH)_4(OZnTp^{Cum,Me})_4$ shift to 563 and 740 nm upon addition of base

(Figure 7), and the color of the solution changes from the characteristic green of many phthalocyanine complexes to dark blue (Table 2). The spectral changes that occur in the visible have accompanying changes in the Soret as the three bands at 241, 301, and 320 nm that appear for $NiPc(OH)_4(OZnTp^{Cum,Me})_4$ move to 269 and 324 nm for the deprotonated product. A transition that appears at 230 nm for both compounds is associated with the $Tp^{Cum,Me}$ ligand. Bands in the Soret region have been assigned as in-plane NiPc transitions, while intense bands in the 400 and 600 nm regions are $n \rightarrow \pi^*$ and $\pi \rightarrow \pi$, respectively.[10] The lower energy transitions appear to be more sensitive to Lewis acid coordination to peripheral oxygen atoms than transitions in the Soret region.

In the absence of crystals of the blue product that are suitable for structural characterization, ^1H NMR has been used to obtain information about $ZnTp^{Cum,Me}$ coordination to the ring oxygens. Sharp resonances at 8.26 and 3.04 ppm appear for phthalocyanine ring protons and NMe_4^+ cations, respectively, with integration factors that are consistent with the $(NMe_4)_4[NiPc(O_2ZnTp^{Cum,Me})_4]$ formulation for the blue product. Resonances for the methylcumenylpyrazolyl groups appear broadened and similar to the resonances of $[ZnTp^{Cum,Me}(PhtCat)]^-$. As with the model anion, proton resonances for the 2 and 6 cumenyl ring protons appear as a slightly broadened doublet, but the 3 and 5 ring protons appear as a broad singlet. Similarities in features of the NMR spectra, the red shift in visible transitions upon complete deprotonation, and the structural resemblance of catecholate regions of the phthalocyanine ring to $[ZnTp^{Cum,Me}(PhtCat)]^-$ point to the conclusion that the Zn centers move into chelated coordination sites about the ring (**III**).

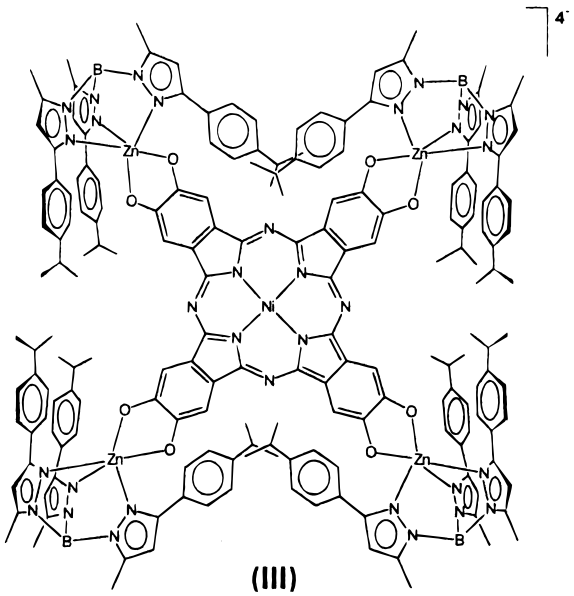

(III)

Deprotonated catecholate ligands are subject to aerobic oxidation. As a test for potential ring oxidation, a dichloromethane solution containing the deprotonated product was treated with dilute HCl. The solution returned to the green color of $NiPc(OH)_4(OZnTp^{Cum,Me})_4$, and the optical spectrum of the solution contained transitions that appear characteristically for the partially protonated product. A similar procedure carried out in methanol gave $NiPc(OH)_8$ and $Tp^{Cum,Me}ZnCl$ as hydrolysis products. These results confirm that the red shift in phthalocyanine bands is associated with complete deprotonation of ring catechol functionalities and not aerobic redox chemistry at deprotonated ring catecholate sites.

Conclusions

Demethylation of $NiPc(OMe)_8$ provides a simple, convenient route to $NiPc(OH)_8$. Catechol functionalities of $NiPc(OH)_8$ offer an opportunity for study of metal chelation to peripheral sites that are directly conjugated with the phthalocyanine ring. The addition of $Si(t\text{-}Bu)Me_2Cl$ to the ring oxygens of $NiPc(OH)_8$ has been used to prepare a unique silyloxylated phthalocyanine, $NiPc(OSi(t\text{-}Bu)Me_2)$, as a soluble precursor to $NiPc(OH)_8$ and to other functionalized phthalocyanines. 5,6-Dihydroxyphthalimide ($H_2PhtCat$) has been used as a simple model for the coordination of transition metals to the catechol functionalities of $NiPc(OH)_8$. Structural characterization on $Tp^{Cum,Me}Zn(HPhtCat)$ and $(NMe_4)[Tp^{Cum,Me}Zn(PhtCat)]$ has shown how the $Tp^{Cum,Me}Zn$ unit may bond at partially protonated and fully deprotonated catecholate sites of $NiPc(OH)_8$. ^1H NMR spectra indicate that arms of the $Tp^{Cum,Me}$ ligand undergo rapid dissociative site exchange for $Tp^{Cum,Me}Zn(HPhtCat)$, but slower exchange leading to broadened resonances for $[Tp^{Cum,Me}Zn(PhtCat)]^-$ with the chelated catecholate ligand. The addition of $Tp^{Cum,Me}Zn(OH)$ to $NiPc(OH)_8$ occurs with stoichiometric deprotonation to give $NiPc(OH)_4(OZnTp^{Cum,Me})_4$. Structural characterization has shown that two trans catechol sites chelate with Zn atoms, and the two remaining sites coordinate through single oxygens. The features of coligands bonded to peripheral metals may be used to form stereoselective substrate binding sites at the central metal. Further addition of base appears to complete ring deprotonation and, from similarities in the NMR spectrum of $[Tp^{Cum,Me}Zn(PhtCat)]^-$, lead to chelation to peripheral catecholate oxygens. Complete deprotonation is accompanied by a color change and large low-energy shifts of bands in the visible region of the phthalocyanine spectrum.

Acknowledgment. We thank Jarral Ryter and Dr. William Durfee for their help in developing early stages of this project. Support for this research came from the National Science Foundation and the Cristol Fund. M.R. would like to thank the Deutsche Forschungsgemeinschaft for a postdoctoral research fellowship.

Supporting Information Available: X-ray crystallographic files in CIF format for $NiPc(OSi(t\text{-}Bu)Me_2)_8 \cdot 2CHCl_3$, $ZnTp^{Cum,Me}(HPhtCat) \cdot MeOH \cdot 1.5CH_2Cl_2$, $(NMe_4)[ZnTp^{Cum,Me}(PhtCat)] \cdot 2.75MeOH$, $NiPc(OH)_4(OZnTp^{Cum,Me})_4 \cdot 3CH_3CN$, and $NiPc(OH)_4(OZnTp^{Cum,Me})_4 \cdot 2CH_2Cl_2 \cdot 4.5CH_3CN$ are available on the Internet only. Access information is given on any current masthead page.

IC980036G